

# AN INTEGRATED ACTIVE-RC POWERLINE NOTCH FILTER FOR BIOPOTENTIAL ACQUISITION DEVICES

Hussain Alzaher, Noman Tasadduq and Yaqub Mahnashi

*Electrical Engineering Department, King Fahd University of Petroleum & Minerals, 31261, Dhahran, Saudi Arabia*

**Keywords:** Notch filter, CMOS Analog integrated circuits, Biomedical.

**Abstract:** An integrable 60Hz continuous time active-RC notch filter is presented. This is made possible through replacing passive resistors by R-2R ladders providing area saving of approximately 120 times. The proposed filter is to be embedded into instrumentation amplifier for biopotential measuring devices. Simulation results of a fully differential 4<sup>th</sup>-order filter show notch depth of 68dB and THD of better than -70dB while consuming 18 $\mu$ W.

## 1 INTRODUCTION

Very low frequency filters has wide range of applications in biomedical signal processing (Li, Poon and Zhang, 2010). In particular, it is desired to eliminate power line frequency disturbance of 60Hz (50Hz in Europe) from the measured signal using notch filters. Power line interference is the most common problem in the detection and processing of biopotential signals (Qian et al., 2005; Ling et al., 2007; Ling and Luo, 2008; Ma et al., 2009; Ma et al., 2009). Despite the use of differential amplification methods and active body potential driving to eliminate the common-mode signals, the line frequency interference occurs in the important frequency range where biopotentials and other physiological signals have most of their energy. This is the case in electroencephalogram (EEG), electrocardiogram (ECG), and electromyogram (EMG) recordings. Power line interference has considerable effect and plays an important part on the quality of these signals.

In order to utilize very large-scale integration (VLSI) techniques in biomedical instrumentation, implementation of this 60Hz notch filter in a single integrated chip (IC) is required. This has been a challenging design problem due to the difficulty in developing efficient methods to achieve large time constant using integrated passive elements. Several different techniques have been used to circumvent this problem. A 5<sup>th</sup> order elliptic lowpass notch filter using LC ladder approach based on OTAs was

reported in Qian et al. (2005), Ling et al. (2007) and Ling et al. (2008). Current division and current cancellation techniques are employed for the designing ultra-low (in order of nA/V or pA/V) transconductance with transistors working in weak inversion region for low power operation enabling the use of small capacitor values. The single ended filter of Qian et al. (2005) is fabricated in 0.35 $\mu$ m CMOS process, and achieves 66dB notch attenuation at 50Hz with a stopband attenuation of 36dB above 50Hz, while consuming total power of 11.1 $\mu$ W. But it is associated with THD of -50dB for an input voltage of 25mV and frequency of 8Hz. Whereas, the filter of Ling et al. (2007) and Ling et al. (2008) is simulated using 0.6 $\mu$ m CMOS process, and achieves 58.5dB attenuation at 50Hz with a stopband attenuation of 32dB above 50Hz.

Switched-capacitor (SC) based low frequency filters in modern IC processes suffer from leakage problem and hence the sample-hold circuits of the switched based topologies are unsuitable for applications requiring large time constants (of the order of millisecond or more) (Li et al., 2010). On the other hand, gm-C based filters are usually associated with limited linearity. In general, design of OTAs turned to be challenging under constrains of low-noise performance, dynamic range and chip area. This is because a small transconductance requires reducing the biasing current which automatically results in smaller input linear range and more noise. The low linearity associated with the use of transconductors is overcome by a rare

active RC opamp based filter presented in Casper, Comer and Comer (1999). It utilizes time constant multiplier (TCM) circuit to attain large time constants using resistors and capacitors that can be integrated. The filter typically exhibits Q of 1/2, and a notch depth of 45dB. But the suggested circuit uses 10 opamps and thus the power consumption is expected to be large.

This paper presents a new CMOS circuit technique for implementing a continuous time 60Hz notch filter suitable for integration. A new filter design approach maintaining the advantages of existing techniques while providing improved characteristics is developed. The following section presents the proposed filter. Design of the different components of the filter is presented in section 3. Simulation results are given in section 4.

## 2 PROPOSED APPROACH

Active-RC filters inherently exhibit high dynamic ranges and the required large time constants can be realized with the help of R-2R ladders (usually used in data converters). The R-2R ladder, shown in Figure 1, can be considered as a digitally programmable resistor given by:

$$R_{eq} = \frac{V}{I} = \beta R \quad \text{where} \quad \beta = \frac{1}{\sum_{i=1}^n b_i 2^{-i}} \quad (1)$$

where  $b_i$ , equaling 0 or 1, is the  $i^{th}$  bit in an n-bit digital control word. However, the optimum use of R-2R ladders in this application occurs when their configurations result in the largest possible equivalent resistance, between the input terminal of a ladder and virtual ground.

The maximum equivalent resistance, of an R-2R ladder is achieved only when the least significant branch current ( $I_{LS}$ ) is connected to the virtual ground (i.e  $b_n=1$  and others  $b_i=0$ ). Therefore, the maximum equivalent resistance  $R_{max} = 2^n R$  can be increased by increasing the size of the ladder (n) and/or the value of the basic resistance R. In this case there is no need to use any switch. Also, since the value of  $I_{LS}$  is independent of the 2R resistance connected with  $b_1$ , it can be removed to save more area. Thus, the total area needed to make an n-bit R-2R reduces to  $R_{tot}=(3n-1)R$ . The relative saving in area achieved through the use of a R-2R ladder is proportional to  $R_{max}/R_{tot}=2^n/(3n-1)$ . Therefore, it can be seen that this saving is independent of R values and it improves considerably as n increases. For example, saving in area of approximately 11, 20, 35, 117 and 400 times is achieved for n= 8, 10, 12, and 14, respectively.

In conventional use of R-2R in data conversion, the main error sources are due to the switch-on resistances which are avoided in our proposed solution. The R-2R ladder can be incorporated by replacing the passive resistors of the original filter as long as these resistors are connected to virtual ground, which simulates the proper operating condition of the R-2R ladder. The Tow-Thomas

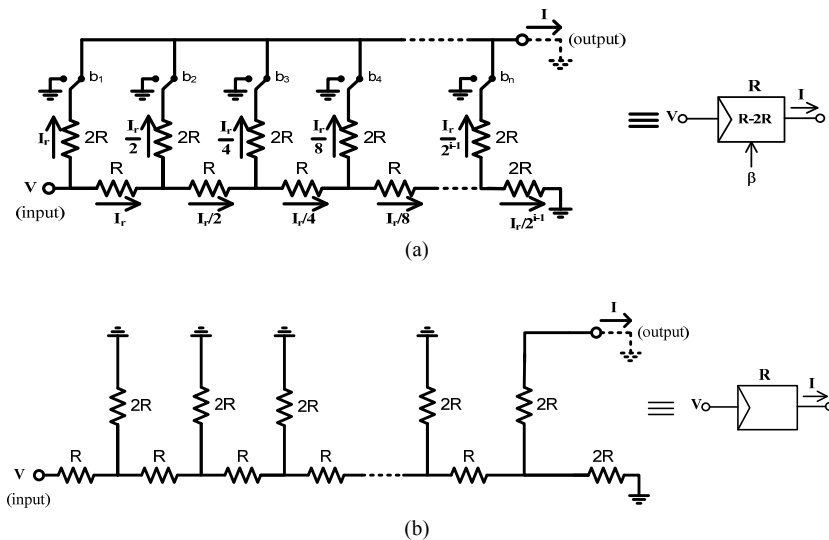


Figure 1: R-2R ladder (a) conventional (b) for this application.

filter topology exhibits this feature and can be designed for pre-required gain and  $Q$  and hence, is selected for this application. The proposed filter is shown in Figure 2.

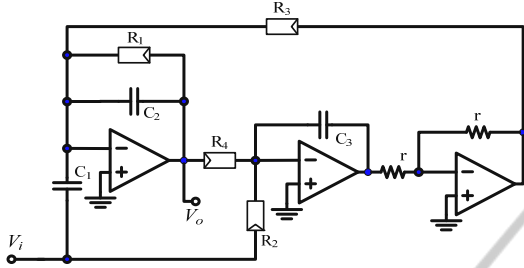


Figure 2: Single ended version of the proposed filter.

Assuming finite opamp gains of  $A$  and with the practical convenient choice of  $R_2=R_3=R_4=R$ ;  $C_1=C_2=C$ ;  $R_1=qR$  non-ideal analysis of the circuit of Figure 3 yields the following transfer function:

$$T_{(non-ideal)}(s) = \frac{V_o}{V_i} \approx - \frac{s^2 + s \left( \frac{2}{C_3 R A} \right) + \frac{1}{C C_3 R^2}}{s^2 + s \left( \frac{2}{C_3 R A} + \frac{1}{C q R} + \frac{2}{C R A} \right) + \left( \frac{1}{C C_3 R^2} \right)} \quad (2)$$

The non-ideal parameters of the filter will be given by:

$$\omega_{o(non-ideal)}^2 \approx \omega_o^2 = \frac{1}{C C_3 R^2} \quad (3)$$

$$\begin{aligned} \Rightarrow Q_{(non-ideal)} &\approx \frac{1}{\frac{1}{C q R} + \frac{2}{A} \left( \frac{1}{C_3} + \frac{1}{C} \right)} \times \frac{1}{R \sqrt{C C_3}} \\ &= Q \frac{1}{1 + \frac{2q}{A} \left( \frac{C}{C_3} + 1 \right)} \end{aligned} \quad (4)$$

The depth of the notch will be given by:

$$\begin{aligned} p &= \frac{1}{|T_{(non-ideal)}(j\omega_o)|} = 1 + \frac{C_3}{C} \left( \frac{A}{2q} + 1 \right) \\ &= 1 + \sqrt{\frac{C_3}{C}} \left( \frac{A}{Q} + \sqrt{\frac{C_3}{C}} \right) \end{aligned} \quad (5)$$

Therefore,  $p$  can be increased by increasing the ratio  $C_3/C$ ,  $A$  and/or decreasing  $Q$ . In practice and for any notch filter there is inverse relation between the depth of the notch  $p$  and  $Q$ . This result is clearly

shown in (5). On the other hand, it is clear from (4) and (5) that as  $A$  increases  $p$  will increase and  $Q_{(non-ideal)}$  will slightly increase to approach its ideal value. Also, increasing the ratio  $C_3/C$  will have more impact on increasing  $p$  than decreasing  $Q$ . Hence it is advantageous to select  $C_3/C$  as large as possible.

Mismatches of passive resistance within each ladder will cause error in value of  $R_{eq}$ . This would cause the notch frequency to deviate from its nominal value. Thus, some sort of fine tuning is needed to compensate for passive elements variation. Considering (3)-(4), it can be seen that  $\omega_o$  can be tuned without disturbing  $Q$  via adjusting either all resistors  $R$ 's and/or all capacitors simultaneously. Fine tuning can be achieved using resistors and/or capacitor matrices. Three 6-bit capacitor matrices are adopted to tune the filter notch frequency. Tuning range from 40Hz to 80Hz for notch frequency is selected. This allows for compensating for  $\pm 33.3\%$  variation in nominal frequency, achieving resolution accuracy of approximately 1% (0.6Hz).

### 3 IMPLEMENTATION

Fully integrated biomedical systems incorporate fully differential architectures to enhance the performance in terms of supply noise rejection, signal swing, and harmonic distortion and also to reduce the effect of coupling between various blocks. Also in fully differential structure, there is no need for the inverter since signals can be inverted by means of proper cross coupling between the positive and negative paths. A fully differential version of a two stage class AB opamp is shown in Figure 3 (Morillo et al., 2006). Since both input and output stages are class-AB, it can work with very low biasing currents, hence providing very low power solution.

The opamp was simulated using supply voltages of  $\pm 0.75V$ . The opamp was optimized to achieve at least 70dB gain with minimum biasing current while deriving load capacitances of 50pF and resistances of 80k $\Omega$ . This load represents the most stringent load ( $C_3$  and ladder of  $R_3$ ) derived by the second opamp. The optimization process has resulted in a gain of 72dB when the opamp is biased with a total current of 3 $\mu A$ . The opamp is compensated to have a phase margin of better than 65 $^\circ$  resulting in a unity gain frequency ( $f_i$ ) of 90kHz.

The other major step in the implantation phase is to decide on the ladder size and value of passive

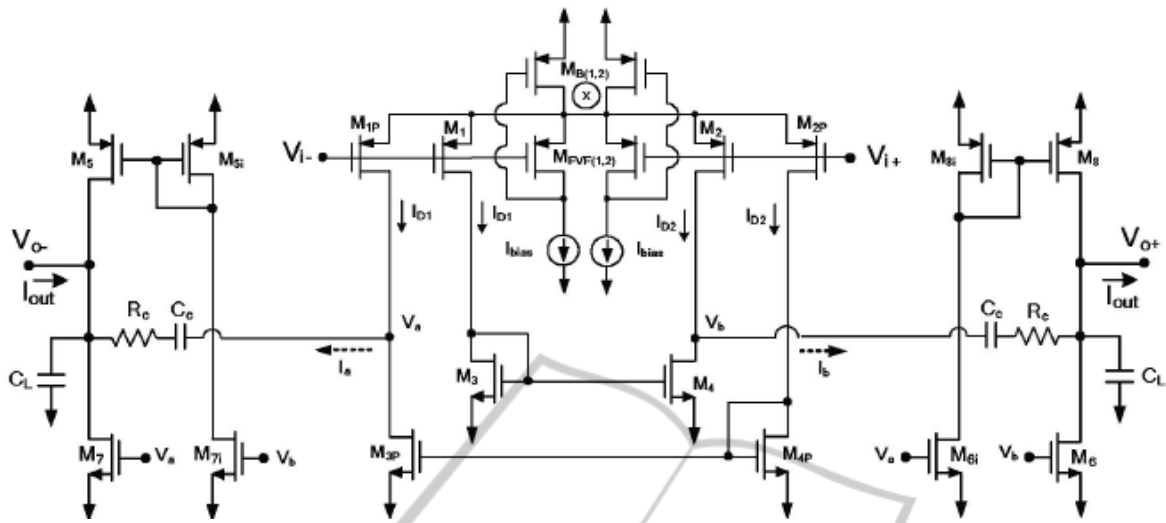


Figure 3: A two stage class-AB opamp (Morillo et al., 2006).

components required to develop the proposed filter. The value of CR required to achieve 60Hz notch frequency can be determined for a specific ladder size and  $C_3$ . Assuming maximum capacitance of 50pF for  $C_3$  and  $R=40k\Omega$ , Table 1 gives the required value of  $C=C_1=C_2$  for several ladder sizes. Also, the value of  $qR$  for maintaining  $Q=1/2$  is given.

It is found that the minimum area is achieved for the case of 12 bits wherein the passive components are  $C_3=50pF$ ,  $C_1=C_2=5.2pF$ ,  $R=40k\Omega$  and  $qR=62k\Omega$ . Table 2 shows the several different values of  $C_3$  and  $C$  for achieving notch frequency of 60Hz when using 12 bit ladders of  $R=40k\Omega$ . Also, it gives the required values of  $qR$  to adjust  $Q$  to  $1/2$ . Effect of increasing  $C_3$  to improve the notch depth for a fixed  $Q$  of  $1/2$  is verified through simulation. It has been found that as  $C_3$  is increased, more depth is attained. In fact selecting  $C_3=50pF$  (assuming maximum capacitance of 50pF) shows a 10dB improvement in the notch depth compared with the case of equal capacitors.

Table 1: Passive component values as function of various ladder sizes.

$C_3$	$C=C_1=C_2$	$qR$
50pF	5.2pF	62k $\Omega$
40pF	6.5pF	49.6k $\Omega$
30pF	8.7pF	37.2k $\Omega$
20pF	13pF	24.8k $\Omega$
16.1pF	16.1pF	20k $\Omega$

Table 2: Several possible values of  $C_3$  for  $Q=1/2$ ,  $R=40k\Omega$ .

$C_3$	$C=C_1=C_2$	$qR$
50pF	5.2pF	62k $\Omega$
40pF	6.5pF	49.6k $\Omega$
30pF	8.7pF	37.2k $\Omega$
20pF	13pF	24.8k $\Omega$
16.1pF	16.1pF	20k $\Omega$

#### 4 SIMULATION RESULTS

Post layout simulations are carried out using 0.18 $\mu$ m CMOS technology for the proposed filter. The filter uses a supply voltage of  $\pm 0.75V$  while consuming total power of 9 $\mu$ W while occupying an area of 0.25 mm<sup>2</sup>. The  $R_1$  ladders were made up of 14-bit, the additional 2 bits are employed to allow programming the quality factor of the filter from 1/2 to 2. Post layout simulation results show that the filter achieves notch attenuation of 43dB and  $Q$  of approximately  $1/2$  as shown in Figure 4. The notch frequency can be tuned from approximately 40Hz to 80Hz which represents more than  $\pm 33\%$  variations of the nominal value of 60Hz as shown in Figure 4 using capacitor arrays. Also, it was found that the gain of the high passband filter is flat for frequencies up to approximately 100kHz because of the relatively low unity gain frequency of the opamp. Two sections of the filter were connected in cascade to realize 4th-order design in order to enhance the notch depth. Simulation results are shown in Figure 5 where -78dB notch depth is recorded.

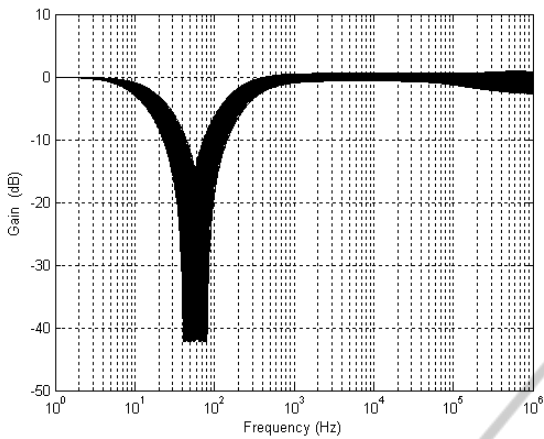


Figure 4: Frequency response of the proposed filter.

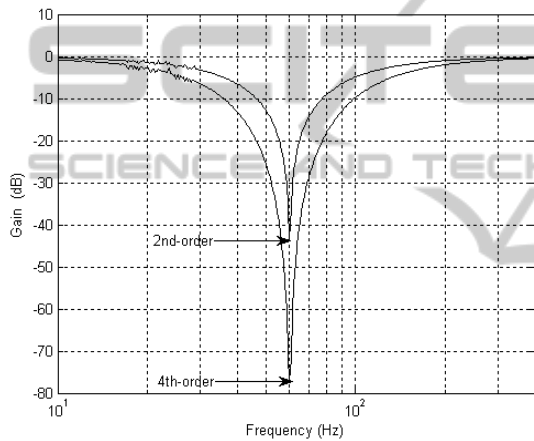


Figure 5: Simulation results of the 2<sup>nd</sup>-order filter and cascaded 4<sup>th</sup>-order filter.

It is found that the maximum output signal peak to peak voltage before clipping is approximately 1.2V. Also, total harmonic distortion (THD) of better than -70dB is achieved. The third-order intermodulation distortion is found using two tone tests with frequencies at 40Hz and 50Hz. It is found that the filter exhibits IIP3 of about 49dBm as shown in Figure 6. The input referred noise root spectral density of the filter is shown in Figure 7. The total noise power is found to be approximately 280 $\mu$ V (-58dBm) over low frequency passband (up to 60Hz). The corresponding spurious-free dynamic range (SFDR) can be found from the IIP3 and noise power (N):

$$SFDR = \frac{2}{3}(IIP3 - N) \quad (6)$$

This leads to SFDR of approximately 71.3dB (referenced to 50 $\Omega$ ).

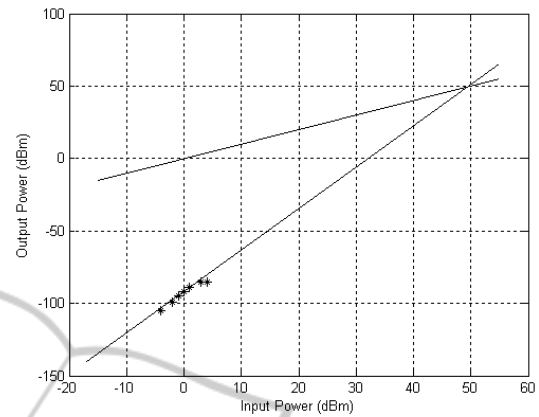


Figure 6: Estimation of IP3 using two tone tests.

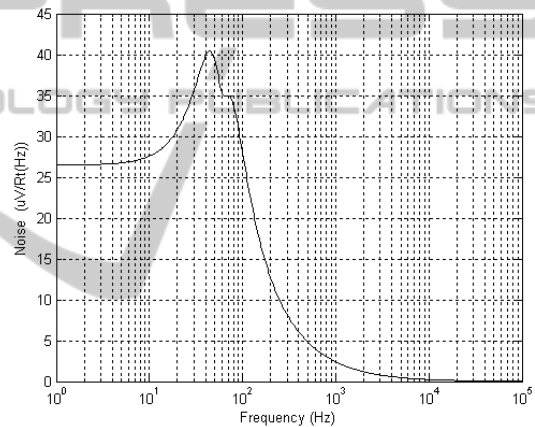


Figure 7: Input referred noise root spectral density.

In addition, when  $Q=2$  a notch depth of -36dB is achieved. It is found that by cascading two of these sections the low side passband frequency extends up to 60Hz and the notch depth becomes about -68dB. Table II shows a summary of the performance of the proposed filter along with various filters in the literature.

It is clear that the proposed filter achieves much lower power consumption compared with that of Ma et al. (2009). Also, it manages to show 20dB improvement over its counterpart of Qian et al. (2005) in terms of THD. For the case of  $Q=1/2$ , the 4<sup>th</sup>-order filter provides 12dB notch depth more than Qian et al. (2005) while using 15% less power (since single-ended filters typically often require one-half the power of their fully differential counterparts).

Table 3: Summary of various filters used for biomedical applications.

Ref.	Qian et al. (2005)	Ling et al. (2007) Ling et al. (2008)	Ma et al. (2009)	This Work
Tech.	0.35 $\mu$ CMOS	0.6 $\mu$ CMOS	90n CMOS	0.18 $\mu$ CMOS
App.	EEG	EEG	Power Line Interference	Power Line Interference
Type	LPN	LPN	Notch	Notch
Order	5	5	-	4
Pole/center frequency	30-67Hz	30-67Hz	50 to 60Hz	60Hz
Power/ Supply Voltage	11 $\mu$ W/ $\pm$ 1.5V	-	75 $\mu$ W/ 3V	18 $\mu$ W/ $\pm$ 0.75V
Structure	OTA-C	OTA-C	Chopper	Opamp
THD	-50dB	-	-	-70dB
Results	Experimental	Simulation	Simulation	Simulation

## 5 CONCLUSIONS

A new fully integrated 60Hz notch filter is proposed. R-2R ladders are adopted to allow the realization of large time constant in small area and they are employed in a proper filter topology. The proposed filter can be easily reconfigured as lowpass, bandpass or highpass filter to meet the specification of other biomedical applications. Simulation results of the filter based on the low-power opamp show comparable power consumption with the gm-C based filter while achieving better linearity.

## ACKNOWLEDGEMENTS

The authors would like to thank King Abdulaziz City for Science and Technology (KACST) for the financial support (Project No: AT-29-99).

## REFERENCES

Li, Y., Poon, CY., Zhang, Y., 2010. Analog Integrated Circuits Design for Processing Physiological Signals. *IEEE Reviews on Biomedical Eng.*, 3, 93-105.

- Qian, XB., Xu,YP., Li, XP., 2005. A CMOS Continuous-Time Lowpass Notch Filter for EEG Systems. *Analog Integrated Circuits Signal Processing*. 44(3), 231–238.
- Ling, C., Ye, P., Liu, R., Wang, J., 2007. A Low-Pass Power Notch Filter Based on an OTA-C Structure for Electroencephalogram. *Proc. International Symposium on Intelligent Signal Processing and Comm. Syst. China*, 451-453.
- Ling, C., Luo, M., 2008. Research of the ASIC Used for EEG Signal Detecting. *Int. Conf. on Anti-counterfeiting, Security and Identification (ASID) China*, 316-319.
- Ma, C., Mak, P., Vai, M., Mak, P., Pun, S., Feng, W., Martins, RP., 2009a. Frequency-Bandwidth-Tunable Powerline Notch Filter for Biopotential Acquisition Systems. *Electronics Letters*, 45(4), 197-199.
- Ma, C., Mak, P., Vai, M., Mak, P., Pun, S., Feng, W., Martins, R P., 2009b. A 90nm CMOS Bio-Potential Signal Readout Front-End with Improved Powerline Interference Rejection. *IEEE Int. Symp. Circuits Syst. (ISCAS)*, 665-668.
- Casper, BK., Comer, DJ., Comer, DT., 1999. An Integrable 60-Hz Notch Filter. *IEEE Trans. on circuits and systems-II*, 46(1), 74-77.
- Lopez-Morillo, E., Carvajal, RG., ElGimili, H., Lopez-Martin, A., Ramirez-Angulo, J., Rodriguez-Villegas, E., 2006. A very low-power class AB/AB op-amp based sigma-delta modulator for biomedical applications. *Midwest Symposium on Circuits and Systems (MWSCAS'06)*, 2, 458–462.